Table 1
Frequencies of ALS patients with *C9orf72* and *SOD1* mutations in different countries

Study	Population	*C9orf72*			*SOD1*	
		Familial ALS	Sporadic ALS	Mean AAO (range), years	Familial ALS	Sporadic ALS
This study, 2012	Japanese (JaCALS)	0% (0/11)	0.4% (2/552)	64.7 (57–72)	NA	NA
Akimoto et al. (2011)	Japanese (JaCALS)	NA	NA	NA	NA	1.6% (4/255)
DeJesus-Hernandez et al. (2011)	Mixed[a]	23.5% (8/34)	4.1% (8/195)***	54.5 (41–72)	11.8% (4/34)	0% (0/195)
Renton et al. (2011)	Finish	46.4% (52/112)**	21.0% (61/290)***	53 (30–71)	NA	NA
Gijselinck et al. (2012)	Flanders-Belgian	46.7% (7/15)*	4.9% (6/122)***	54.5 (38–64)	0% (0/16)	0% (0/125)
Stewart et al. (2012)	Unknown[b]	27.4% (17/62)	3.6% (6/169)**	58.2 (39–82)	Total 8.2% (19/231)	
Byrne et al. (2012)	Ireland	40.8% (20/49)*	4.9% (19/386)***	56.3 (NA)	Total 0% (0/191)	
Cooper-Knock et al. (2012)	Northern England	42.9% (27/63)*	7.0% (35/500)***	57.3 (27–74)	Total 2.5% (14/563)	
Chiò et al. (2012)	Italian	37.5% (45/120)*	NA	59.0 (NA-80)	0% (0/141)	NA
	Sardinian	57.1% (12/21)**	NA	60.4 (NA)	NA	NA
	German	22.0% (9/41)	NA	56.4 (NA)	NA	NA
Majounie et al. (2012)	England	45.9% (45/98)**	6.8% (62/916)***	NA	NA	NA
	German	21.7% (15/69)	5.2% (22/421)***	NA	NA	NA
	Italian	37.8% (34/90)*	4.1% (19/465)***	NA	NA	NA
	Sardinian	57.9% (11/19)**	7.8% (10/129)***	NA	NA	NA
	USA White	US total 36.2% (59/163)*	5.4% (48/890)***	NA	NA	NA
	USA Hispanic		8.3% (6/72)***	NA	NA	NA
	USA Black		4.1% (2/49)	NA	NA	NA
	Australian	NA	5.3% (14/263)***	NA	NA	NA
	Israeli	21.4% (3/14)	NA	NA	NA	NA
	Indian	NA	0% (0/31)	NA	NA	NA
	Asian	5.0% (1/20)	0% (0/238)	NA	NA	NA
	Pacific islander/Guam	NA	0% (0/90)	NA	NA	NA
Sabatelli et al. (2012)	Italian	NA	3.7% (60/1624)***	58.6 (49–65)	NA	NA
	Sardinian	NA	6.8% (9/133)***	62.9 (58–63)	NA	NA

Key: AAO, age at onset; ALS, amyotrophic lateral sclerosis; JaCALS, Japanese Consortium of Amyotrophic Lateral Sclerosis Research; NA, not available.
[a] Mixed included 229 ALS patients from Mayo Clinic, Florida: White (212), Asian (1), Pacific Islander (1), and Black or African American (15).
[b] Unknown included 231 ALS patients from the ALS Clinic of Vancouver Coastal Health and the University of British Columbia (Vancouver General Hospital and GF Strong Rehabilitation Centre sites).
* $p < 0.05$, compared with our results (2-tailed, Yates's χ^2 test).
** $p < 0.01$, compared with our results (2-tailed, Yates's χ^2 test).
***$p < 0.001$ compared with our results (2-tailed, Yates's χ^2 test).

3.2.4. Subject B-II (family B)

Subject B-II, a sibling of Patient B-I, had a *C9orf72* mutation but did not have symptoms of dementia or motor neuron disease until age 76 (Fig. 1).

4. Discussion

We began this study considering patients without family histories of ALS to be SALS because our cohort included only family histories of ALS but not FTD or PPA. Although it may be difficult to describe the real frequency in SALS because 1 of the SALS patients had a family member who developed PPA, the frequencies of the *C9orf72* mutation in Japanese patients were 0.4% (2/552) in SALS and 0% (0/11) in FALS according to this classification. In contrast, the frequencies of the *C9orf72* mutation fall within the ranges of 21%–57% in FALS and 3%–21% in SALS in Western populations (Table 1), and the *C9orf72* mutation has been reported as the most common genetic cause of FALS and SALS in Western populations (Byrne et al., 2012; Chiò et al., 2012; Cooper-Knock et al., 2012; DeJesus-Hernandez et al., 2011; Gijselinck et al., 2012; Majounie et al., 2012; Renton et al., 2011; Sabatelli et al., 2012; Stewart et al., 2012). However, the *C9orf72* mutation in this study was not more frequent than the *SOD1* mutation in Japanese SALS patients (0.4% and 1.6%, Table 1) (Akimoto et al., 2011). Considering these data, the *C9orf72* mutation is more common than the *SOD1* mutation in Western populations but not in Japan, suggesting different genetic backgrounds. Our results may explain the association study of rs2814707 on 9p21.2, which was reported to be the most significantly associated SNP with SALS in Caucasian but not in Japanese and Chinese populations (Iida et al., 2011). A recent report revealed that the rate of expansion in Asian FALS and SALS was 5% (1/20) and 0% (0/238), respectively (Majounie et al., 2012). An analysis of the SNPs on chromosome 9p revealed that all 4 subjects with the *C9orf72* mutation and another Japanese subject from the previously mentioned report (Majounie et al., 2012) share a shorter region of the risk haplotype

than Western populations. Thus, the haplotype bearing the *C9orf72* mutation was only shared in a narrow region between Western and Asian populations, suggesting that the *C9orf72* mutation may be an old mutation in human migration history from Western to East Asia. This mutation was estimated to be approximately 1500 years old (Majounie et al., 2012).

Bulbar onset and cognitive impairment have been reported to be more common in ALS patients with the *C9orf72* repeat expansion (Chiò et al., 2012; Cooper-Knock et al., 2012; DeJesus-Hernandez et al., 2011; Sabatelli et al., 2012; Stewart et al., 2012). We did not find any patients with bulbar onset, but we identified 2 patients with dementia. Although the age at onset has been known to be lower in SALS patients with the *C9orf72* mutation than in those without this mutation (Sabatelli et al., 2012), our patients exhibited a relatively older age at onset (Table 1).

Although apparently sporadic patients with *C9orf72* mutation have been detected worldwide (Byrne et al., 2012; Cooper-Knock et al., 2012; Sabatelli et al., 2012), it was not known whether this phenomenon was due to incomplete penetrance or to spontaneous expansion of the GGGGCC hexanucleotide repeat from a nonpathogenic parental form (ie, a de novo expansion). In this study, we found a 76-year-old healthy individual with a *C9orf72* mutation (Subject B-II), as described in previous studies (Majounie et al., 2012; Renton et al., 2011). This discovery suggests not de novo expansion but incomplete penetrance, which explains the existence of apparently sporadic patients with the *C9orf72* mutation. Although it has been reported that the penetrance of the *C9orf72* mutation is almost full by 80 years by Kaplan–Meier analysis of 603 mutant gene carriers and 5 neurologically healthy individuals, further studies of family members of patients with the *C9orf72* mutation will be required to calculate the true penetrance and to improve genetic counseling.

Finally, we found a PPA patient with the *C9orf72* mutation after detecting the mutation in a SALS patient, suggesting the importance of collecting information regarding whether SALS patients have a family history of dementia or aphasia. Therefore, the possibility of *C9orf72* mutation should be investigated when clinicians meet with SALS patients after determining their family histories of FTD or PPA. Furthermore, our data supported Byrne and colleagues' suggestion that a family history of FTD should also be included in the revised definition of FALS (Byrne et al., 2012).

Disclosure statement

All of the authors disclose no conflicts of interest. The study was approved by the ethical committees of the participating centers. All participants gave written informed consent.

Acknowledgements

The authors thank all of the participants in this study. The authors also thank Dr. Mariely DeJesus-Hernandez, Dr. Ilse Gijselinck, Dr. Marc Cruts, and Dr. Christine Van Broeckhoven for technical advice. This work was supported by the Ministry of Education, Culture, Sports, Science and Technology of Japan (21229011, 21390272, 21591098, 22790817, 22790829, and 23659452), the Ministry of Welfare, Health and Labor of Japan (20261501, 22140501, 22140901, and CCT-B-1701), the Japan Science and Technology Agency, Core Research for Evolutional Science and Technology, and the Inochinoiro Foundation of Japan.

Appendix A. Members of the Japanese Consortium for Amyotrophic Lateral Sclerosis Research (JaCALS)

Dr. Mitsuya Morita, Dr. Imaharu Nakano (Division of Neurology, Department of Internal Medicine, Jichi Medical University); Dr. Masashi Aoki (Department of Neurology, Tohoku University School of Medicine); Dr. Koichi Mizoguchi (Department of Neurology, Shizuoka Institute of Epilepsy and Neurological Disorders); Dr. Kazuko Hasegawa (Division of Neurology, National Hospital Organization, Sagamihara National Hospital); Dr. Akihiro Kawata (Department of Neurology, Tokyo Metropolitan Neurological Hospital); Dr. Ikuko Aiba (Department of Neurology, National Hospital Organization Higashinagoya National Hospital); Dr. Takashi Imai (Division of Neurology, National Hospital Organization, Miyagi National Hospital); Dr. Koichi Okamoto (Department of Neurology, Gunma University Graduate School of Medicine); Dr. Koji Abe (Department of Neurology, Okayama University Graduate School of Medicine); and Dr. Hirohisa Watanabe, Dr. Mizuki Ito, Dr. Jo Senda (Department of Neurology, Nagoya University Graduate School of Medicine).

Appendix B. Supplementary data

Supplementary data associated with this article can be found, in the online version, at http://dx.doi.org/10.1016/j.neurobiolaging.2012.05.011.

References

Akimoto, C., Morita, M., Atsuta, N., Sobue, G., Nakano, I., 2011. High-Resolution Melting (HRM) Analysis of the Cu/Zn Superoxide Dismutase (SOD1) Gene in Japanese Sporadic Amyotrophic Lateral Sclerosis (SALS) Patients. Neurol. Res. Int. 2011, 165415.

Brooks, B.R., Miller, R.G., Swash, M., Munsat, T.L., 2000. El Escorial revisited: revised criteria for the diagnosis of amyotrophic lateral sclerosis. Amyotroph. Lateral Scler. Other Mot. Neuron Disord. 1, 293–299.

Byrne, S., Elamin, M., Bede, P., Shatunov, A., Walsh, C., Corr, B., Heverin, M., Jordan, N., Kenna, K., Lynch, C., McLaughlin, R.L., Iyer, P.M., O'Brien, C., Phukan, J., Wynne, B., Bokde, A.L., Bradley, D.G., Pender, N., Al-Chalabi, A., Hardiman, O., 2012. Cognitive and clinical characteristics of patients with amyotrophic lateral sclerosis carrying a C9orf72 repeat expansion: a population-based cohort study. Lancet Neurol. 11, 232–240.

Chiò, A., Borghero, G., Restagno, G., Mora, G., Drepper, C., Traynor, B.J., Sendtner, M., Brunetti, M., Ossola, I., Calvo, A., Pugliatti, M., Sotgiu, M.A., Murru, M.R., Marrosu, M.G., Marrosu, F., Marinou, K., Mandrioli, J., Sola, P., Caponnetto, C., Mancardi, G., Mandich, P., La Bella, V., Spataro, R., Conte, A., Monsurrò, M.R., Tedeschi, G., Pisano, F., Bartolomei, I., Salvi, F., Lauria Pinter, G., Simone, I., Logroscino, G., Gambardella, A., Quattrone, A., Lunetta, C., Volanti, P., Zollino, M., Penco, S., Battistini, S., Renton, A.E., Majounie, E., Abramzon, Y., Conforti, F.L., Giannini, F., Corbo, M., Sabatelli, M., ITALSGEN consortium, 2012. Clinical characteristics of patients with familial amyotrophic lateral sclerosis carrying the pathogenic GGGGCC hexanucleotide repeat expansion of C9ORF72. Brain 135, 784–793.

Cooper-Knock, J., Hewitt, C., Highley, J.R., Brockington, A., Milano, A., Man, S., Martindale, J., Hartley, J., Walsh, T., Gelsthorpe, C., Baxter, L., Forster, G., Fox, M., Bury, J., Mok, K., McDermott, C.J., Traynor, B.J., Kirby, J., Wharton, S.B., Ince, P.G., Hardy, J., Shaw, P.J., 2012. Clinico-pathological features in amyotrophic lateral sclerosis with expansions in C9ORF72. Brain 135, 751–764.

DeJesus-Hernandez, M., Mackenzie, I.R., Boeve, B.F., Boxer, A.L., Baker, M., Rutherford, N.J., Nicholson, A.M., Finch, N.A., Flynn, H., Adamson, J., Kouri, N., Wojtas, A., Sengdy, P., Hsiung, G.Y., Karydas, A., Seeley, W.W., Josephs, K.A., Coppola, G., Geschwind, D.H., Wszolek, Z.K., Feldman, H., Knopman, D.S., Petersen, R.C., Miller, B.L., Dickson, D.W., Boylan, K.B., Graff-Radford, N.R., Rademakers, R., 2011. Expanded GGGGCC Hexanucleotide Repeat in Noncoding Region of C9ORF72 Causes Chromosome 9p-Linked FTD and ALS. Neuron 72, 245–256.

Deng, H.X., Chen, W., Hong, S.T., Boycott, K.M., Gorrie, G.H., Siddique, N., Yang, Y., Fecto, F., Shi, Y., Zhai, H., Jiang, H., Hirano, M., Rampersaud, E., Jansen, G.H., Donkervoort, S., Bigio, E.H., Brooks, B.R., Ajroud, K., Sufit, R.L., Haines, J.L., Mugnaini, E., Pericak-Vance, M.A., Siddique, T., 2011. Mutations in UBQLN2 cause dominant X-linked juvenile and adult-onset ALS and ALS/dementia. Nature 477, 211–215.

Gijselinck, I., Van Langenhove, T., van der Zee, J., Sleegers, K., Philtjens, S., Kleinberger, G., Janssens, J., Bettens, K., Van Cauwenberghe, C., Pereson, S., Engelborghs, S., Sieben, A., De Jonghe, P., Vandenberghe, R., Santens, P., De Bleecker, J., Maes, G., Bäumer, V., Dillen, L., Joris, G., Cuijt, I., Corsmit, E., Elinck, E., Van Dongen, J., Vermeulen, S., Van den Broeck, M., Vaerenberg, C., Mattheijssens, M., Peeters, K., Robberecht, W., Cras, P., Martin, J.J., De Deyn, P.P., Cruts, M., Van Broeckhoven, C., 2012. A C9orf72 promoter repeat expansion in a Flanders-Belgian cohort with disorders of the frontotemporal lobar degeneration-amyotrophic lateral sclerosis spectrum: a gene identification study. Lancet Neurol. 11, 54–65.

Iida, A., Takahashi, A., Deng, M., Zhang, Y., Wang, J., Atsuta, N., Tanaka, F., Kamei, T., Sano, M., Oshima, S., Tokuda, T., Morita, M., Akimoto, C., Nakajima, M., Kubo, M., Kamatani, N., Nakano, I., Sobue, G., Nakamura, Y., Fan, D., Ikegawa, S., 2011. Replication analysis of SNPs on 9p21.2 and 19p13.3 with amyotrophic lateral sclerosis in East Asians. Neurobiol. Aging 32, e713–e754.

International HapMap Consortium, 2003. The International HapMap Project. Nature 426, 789–796.

Laaksovirta, H., Peuralinna, T., Schymick, J.C., Scholz, S.W., Lai, S.L., Myllykangas, L., Sulkava, R., Jansson, L., Hernandez, D.G., Gibbs, J.R., Nalls, M.A., Heckerman, D., Tienari, P.J., Traynor, B.J., 2010. Chromosome 9p21 in amyotrophic lateral sclerosis in Finland: a genome-wide association study. Lancet Neurol. 9, 978–985.

Lomen-Hoerth, C., Anderson, T., Miller, B., 2002. The overlap of amyotrophic lateral sclerosis and frontotemporal dementia. Neurology 59, 1077–1079.

Majounie, E., Renton, A.E., Mok, K., Dopper, E.G., Waite, A., Rollinson, S., Chiò, A., Restagno, G., Nicolaou, N., Simon-Sanchez, J., van Swieten, J.C., Abramzon, Y., Johnson, J.O., Sendtner, M., Pamphlett, R., Orrell, R.W., Mead, S., Sidle, K.C., Houlden, H., Rohrer, J.D., Morrison, K.E., Pall, H., Talbot, K., Ansorge, O., Hernandez, D.G., Arepalli, S., Sabatelli, M., Mora, G., Corbo, M., Giannini, F., Calvo, A., Englund, E., Borghero, G., Floris, G.L., Remes, A.M., Laaksovirta, H., McCluskey, L., Trojanowski, J.Q., Van Deerlin, V.M., Schellenberg, G.D., Nalls, M.A., Drory, V.E., Lu, C.S., Yeh, T.H., Ishiura, H., Takahashi, Y., Tsuji, S., Le Ber, I., Brice, A., Drepper, C., Williams, N., Kirby, J., Shaw, P., Hardy, J., Tienari, P.J., Heutink, P., Morris, H.R., Pickering-Brown, S., Traynor, B.J., Chromosome 9-ALS/FTD Consortium; French research network on FTLD/FTLD/ALS; ITALSGEN Consortium, 2012. Frequency of the C9orf72 hexanucleotide repeat expansion in patients with amyotrophic lateral sclerosis and frontotemporal dementia: a cross-sectional study. Lancet Neurol. 11, 323–330.

Mok, K., Traynor, B.J., Schymick, J., Tienari, P.J., Laaksovirta, H., Peuralinna, T., Myllykangas, L., Chiò, A., Shatunov, A., Boeve, B.F., Boxer, A.L., DeJesus-Hernandez, M., Mackenzie, I.R., Waite, A., Williams, N., Morris, H.R., Simon-Sanchez, J., van Swieten, J.C., Heutink, P., Restagno, G., Mora, G., Morrison, K.E., Shaw, P.J., Rollinson, P.S., Al-Chalabi, A., Rademakers, R., Pickering-Brown, S., Orrell, R.W., Nalls, M.A., Hardy, J., 2012. The chromosome 9 ALS and FTD locus is probably derived from a single founder. Neurobiol. Aging 33, e3–e8.

Neumann, M., Sampathu, D.M., Kwong, L.K., Truax, A.C., Micsenyi, M.C., Chou, T.T., Bruce, J., Schuck, T., Grossman, M., Clark, C.M., McCluskey, L.F., Miller, B.L., Masliah, E., Mackenzie, I.R., Feldman, H., Feiden, W., Kretzschmar, H.A., Trojanowski, J.Q., Lee, V.M., 2006. Ubiquitinated TDP-43 in frontotemporal lobar degeneration and amyotrophic lateral sclerosis. Science 314, 130–133.

Renton, A.E., Majounie, E., Waite, A., Simón-Sánchez, J., Rollinson, S., Gibbs, J.R., Schymick, J.C., Laaksovirta, H., van Swieten, J.C., Myllykangas, L., Kalimo, H., Paetau, A., Abramzon, Y., Remes, A.M., Kaganovich, A., Scholz, S.W., Duckworth, J., Ding, J., Harmer, D.W., Hernandez, D.G., Johnson, J.O., Mok, K., Ryten, M., Trabzuni, D., Guerreiro, R.J., Orrell, R.W., Neal, J., Murray, A., Pearson, J., Jansen, I.E., Sondervan, D., Seelaar, H., Blake, D., Young, K., Halliwell, N., Callister, J.B., Toulson, G., Richardson, A., Gerhard, A., Snowden, J., Mann, D., Neary, D., Nalls, M.A., Peuralinna, T., Jansson, L., Isoviita, V.M., Kaivorinne, A.L., Holtta-Vuori, M., Ikonen, E., Sulkava, R., Benatar, M., Wuu, J., Chiò, A., Restagno, G., Borghero, G., Sabatelli, M., Heckerman, D., Rogaeva, E., Zinman, L., Rothstein, J.D., Sendtner, M., Drepper, C., Eichler, E.E., Alkan, C., Abdullaev, Z., Pack, S.D., Dutra, A., Pak, E., Hardy, J., Singleton, A., Williams, N.M., Heutink, P., Pickering-Brown, S., Morris, H.R., Tienari, P.J., Traynor, B.J., ITALSGEN Consortium, 2011. A Hexanucleotide Repeat Expansion in C9ORF72 Is the Cause of Chromosome 9p21-Linked ALS-FTD. Neuron 72, 257–268.

Sabatelli, M., Conforti, F.L., Zollino, M., Mora, G., Monsurrò, M.R., Volanti, P., Marinou, K., Salvi, F., Corbo, M., Giannini, F., Battistini, S., Penco, S., Lunetta, C., Quattrone, A., Gambardella, A., Logroscino, G., Simone, I., Bartolomei, I., Pisano, F., Tedeschi, G., Conte, A., Spataro, R., La Bella, V., Caponnetto, C., Mancardi, G., Mandich, P., Sola, P., Mandrioli, J., Renton, A.E., Majounie, E., Abramzon, Y., Marrosu, F., Marrosu, M.G., Murru, M.R., Sotgiu, M.A., Pugliatti, M., Rodolico, C., ITALSGEN Consortium, Moglia, C., Calvo, A., Ossola, I., Brunetti, M., Traynor, B.J., Borghero, G., Restagno, G., Chiò, A., 2012. C9ORF72 hexanucleotide repeat expansions in the Italian sporadic ALS population. Neurobiol. Aging, 33, e15-e20.

Stewart, H., Rutherford, N.J., Briemberg, H., Krieger, C., Cashman, N., Fabros, M., Baker, M., Fok, A., DeJesus-Hernandez, M., Eisen, A., Rademakers, R., Mackenzie, I.R., 2012. Clinical and pathological features of amyotrophic lateral sclerosis caused by mutation in the C9ORF72 gene on chromosome 9p. Acta Neuropathol. 123, 409–417.

Ticozzi, N., Tiloca, C., Morelli, C., Colombrita, C., Poletti, B., Doretti, A., Maderna, L., Messina, S., Ratti, A., Silani, V., 2011. Genetics of familial Amyotrophic lateral sclerosis. Arch. Ital. Biol. 149, 65–82.

Valdmanis, P.N., Daoud, H., Dion, P.A., Rouleau, G.A., 2009. Recent advances in the genetics of amyotrophic lateral sclerosis. Curr. Neurol. Neurosci. Rep. 9, 198–205.

Brain Advance Access published February 28, 2013
doi:10.1093/brain/awt029 Brain 2013: Page 1 of 12 | 1
BRAIN
A JOURNAL OF NEUROLOGY

Loss of TDP-43 causes age-dependent progressive motor neuron degeneration

Yohei Iguchi,[1] Masahisa Katsuno,[1] Jun-ichi Niwa,[2] Shinnosuke Takagi,[1] Shinsuke Ishigaki,[1] Kensuke Ikenaka,[1] Kaori Kawai,[1] Hirohisa Watanabe,[1] Koji Yamanaka,[3,4] Ryosuke Takahashi,[5] Hidemi Misawa,[6] Shoichi Sasaki,[7] Fumiaki Tanaka[1,8] and Gen Sobue[1,4]

1 Department of Neurology, Nagoya University Graduate School of Medicine, Nagoya 466-8550, Japan
2 Stroke Centre, Aichi Medical University, Aichi 480-1195, Japan
3 Laboratory for Motor Neuron Disease, RIKEN Brain Science Institute, Wako, Saitama 351-0198, Japan
4 CREST, Japan Science and Technology Agency, 4-1-8, Honcho, Kawaguchi, Saitama 332-0012, Japan
5 Department of Neurology, Kyoto University Graduate School of Medicine, Kyoto 606-8507, Japan
6 Department of Pharmacology, Keio University Faculty of Pharmacy, Tokyo 105-8512, Japan
7 Department of Neurology, Neurological Institute, Tokyo Women's Medical University, Tokyo 162-8666, Japan
8 Department of Neurology and Stroke Medicine, Yokohama City University Graduate School of Medicine, Yokohama 236-0004, Japan

Correspondence to: Gen Sobue
Showa-ku, Nagoya 466-8550,
Japan
E-mail: sobueg@med.nagoya-u.ac.jp

Amyotrophic lateral sclerosis is a devastating, progressive neurodegenerative disease that affects upper and lower motor neurons. Although several genes are identified as the cause of familial cases, the pathogeneses of sporadic forms, which account for 90% of amyotrophic lateral sclerosis, have not been elucidated. Transactive response DNA-binding protein 43 a nuclear protein regulating RNA processing, redistributes to the cytoplasm and forms aggregates, which are the histopathological hallmark of sporadic amyotrophic lateral sclerosis, in affected motor neurons, suggesting that loss-of-function of transactive response DNA-binding protein 43 is one of the causes of the neurodegeneration. To test this hypothesis, we assessed the effects of knockout of transactive response DNA-binding protein 43 in mouse postnatal motor neurons using Cre/loxp system. These mice developed progressive weight loss and motor impairment around the age of 60 weeks, and exhibited degeneration of large motor axon, grouped atrophy of the skeletal muscle, and denervation in the neuromuscular junction. The spinal motor neurons lacking transactive response DNA-binding protein 43 were not affected for 1 year, but exhibited atrophy at the age of 100 weeks; whereas, extraocular motor neurons, that are essentially resistant in amyotrophic lateral sclerosis, remained preserved even at the age of 100 weeks. Additionally, ultra structural analysis revealed autolysosomes and autophagosomes in the cell bodies and axons of motor neurons of the 100-week-old knockout mice. In summary, the mice in which transactive response DNA-binding protein 43 was knocked-out specifically in postnatal motor neurons exhibited an age-dependent progressive motor dysfunction accompanied by neuropathological alterations, which are common to sporadic amyotrophic lateral sclerosis. These findings suggest that transactive response DNA-binding protein 43 plays an essential role in the long term maintenance of motor neurons and that loss-of-function of this protein seems to contribute to the pathogenesis of amyotrophic lateral sclerosis.

Keywords: transactive response DNA-binding protein 43; amyotrophic lateral sclerosis; axonal degeneration; autophagosome

Abbreviations: ALS = amyotrophic lateral sclerosis; FTLD = frontotemporal lobar degeneration; TDP CKO = motor neuron-specific TDP-43 knockout; TDP hCKO = TDP heterozygous CKO

Received July 20, 2012. Revised December 17, 2012. Accepted December 28, 2012.

Introduction

Amyotrophic lateral sclerosis (ALS) is a progressive, fatal neurodegenerative disease that affects upper and lower motor neurons in the brain stem and spinal cord. Although previous studies using animal models of ALS have focused mainly on the toxicity of mutant SOD1, one of the causative genes of familial ALS (ALS1), there are pathophysiological differences between ALS1 and sporadic ALS that accounts for ~90% of ALS. The most striking recent discovery regarding ALS is that transactive response DNA-binding protein 43 (TDP-43) was identified as a major component of ubiquitinated neuronal cytoplasmic inclusions in both sporadic ALS and frontotemporal lobar degeneration (FTLD) (Arai *et al.*, 2006; Neumann *et al.*, 2006). In addition, TDP-43 is a causative gene of familial ALS (ALS10) (Gitcho *et al.*, 2008; Kabashi *et al.*, 2008; Sreedharan *et al.*, 2008; Yokoseki *et al.*, 2008). Taken together, these data suggest that TDP-43 plays a key role in the pathogenesis of sporadic ALS. Although TDP-43 is a nuclear protein, it redistributes to the cytoplasm and forms aggregates in affected neurons of patients with sporadic ALS (Arai *et al.*, 2006; Neumann *et al.*, 2006), suggesting that loss of TDP-43 function underlies sporadic ALS pathogenesis. TDP-43 is known to regulate gene transcription, stability of messenger RNA, and exon splicing through interactions with RNA, heterogeneous nuclear ribonucleoproteins and nuclear bodies (Wang *et al.*, 2004; Ayala *et al.*, 2005; Buratti *et al.*, 2005, 2010; Strong *et al.*, 2007; Polymenidou *et al.*, 2011; Sephton *et al.*, 2011; Tollervey *et al.*, 2011). Knockdown of TDP-43 in neuronal cells inhibits neurite outgrowth and diminishes cell viability (Iguchi *et al.*, 2009), whereas TDP-43 depletion induces apoptosis in HeLa or U2OS cells (Ayala *et al.*, 2008). In addition, *Drosophila* without TDP-43 present deficient locomotive behaviours, reduced life span and anatomical defects at neuromuscular junctions (Feiguin *et al.*, 2009). TDP-43-depleted zebrafish exhibit swimming deficits along with excessive, premature branching and shortened motor axons (Kabashi *et al.*, 2011). Furthermore, TDP-43 knockout mice are embryonic lethal (Kraemer *et al.*, 2010; Sephton *et al.*, 2010; Wu *et al.*, 2010), and postnatal deletion of TDP-43 leads to rapid death with loss of body fat (Chiang *et al.*, 2010). Although these findings indicate that TDP-43 is essential for survival of mice at both embryonic and post-natal stages, the effects of TDP-43 depletion in postnatal mammalian neurons have not been fully elucidated. In the present study, we generated motor neuron-specific TDP-43 knockout (TDP CKO) mice using the Cre/loxP recombination system to investigate the effects of TDP-43 loss on postnatal motor neurons in mice.

Materials and methods

Generation and maintenance of TDP-43 conditional knockout mouse

The targeting construct was designed to insert an Frt-flanked neomycin cassette and a loxP site upstream, and a loxP site downstream of the second exon of the *Tardbp* gene. This construct was electroporated into iTL1 BA1 (C57BL/6 × 129/SvEv) hybrid embryonic stem cells. Correctly targeted embryonic stem cells were injected into recipient blastocysts and chimeric mice were bred with C57BL/6J mice. The resulting En1flox-neo mice were then bred to C57BL/6J mice constitutively expressing Flp recombinase to remove the Frt-flanked neo cassette, generating En1flox offspring. En1flox mutant mice were backcrossed with C57BL/6J mice for at least five generations, and then crossed with VAChT-Cre.Fast mice, which are the most validated mice that specifically express Cre in motor neurons (Misawa *et al.*, 2003). To generate TDP-43 conditional knockout mice, we crossed TDP-43$^{flox/flox}$ mice with TDP-43$^{flox/+}$/VAChT-Cre mice. Finally, we obtained TDP-43$^{flox/flox}$/VAChT-Cre (motor neuron-specific TDP-43 knockout: TDP CKO), TDP-43$^{flox/+}$/VAChT-Cre (TDP heterozygous CKO: TDP hCKO), TDP-43$^{flox/flox}$ and TDP-43$^{flox/+}$ mice. The TDP-43$^{flox/flox}$ mice were then used as control littermates in the present analyses. Mice were kept on a 12-h light/12-h dark cycle, with food and water provided *ad libitum*. All animal experiments were performed in accordance with the National Institutes of Health Guide for the Care and Use of Laboratory Animals and under the approval of the Nagoya University Animal Experiment Committee (Nagoya, Japan).

Neurological and behavioural testing

The control ($n = 21$) and TDP CKO ($n = 20$) mice were subjected to the Rotarod task (Economex Rotarod; Columbus Instruments) weekly as described previously (Katsuno *et al.*, 2002). Grip strength was measured weekly by a grip strength meter (MK-380M, Muromachi kikai Co. LTD). During this test, the mice griped the mesh with four limbs and their tail was pulled backwards. Gait stride was measured from 50 cm of footsteps, and the average value was recorded for each mouse.

Immunofluorescent analysis and immunohistochemistry

For immunofluorescent analysis, we perfused 20 ml of a 4% paraformaldehyde fixative in phosphate buffer (WAKO Corp.) through the left cardiac ventricle of mice deeply anaesthetized with medetomidine (0.3 mg/kg), midazolam (4 mg/kg) and butorphanol (5 mg/kg), interperitoneally. Tissues postfixed overnight in 10% phosphate-buffered formalin were then processed for paraffin embedding. We then deparaffinized 3-μm thick tissue sections and dehydrated them with alcohol. Sections were first microwaved for 20 min in 50 mM citrate buffer (pH 6.0), treated with TNB blocking buffer (PerkinElmer) and incubated overnight with anti-TDP-43 rabbit polyclonal antibody (1:1000, ProteinTech), anti-choline-acetyltransferase (ChAT) goat polyclonal antibody (1:100, Milipore), anti-microtubule-associated protein 1 light chain 3 (LC3) mouse monoclonal antibody (1:1000, MBL), phosphorylated neurofilament-H (pNF-H) mouse monoclonal antibody (SMI31) (1:1000, Covance), or anti-neuronal nuclei (NeuN) mouse monoclonal antibody (1:100, Millipore). After washing, for the ChAT staining, sections were incubated with biotinylated donkey anti-goat IgG (1:300, Vector Lab.) for 30 min, washed and incubated with streptavidin conjugated with Alexa Fluor® 546 (1:1000, Invitrogen) for 30 min. For the other antigens, sections were incubated with the indicated secondary antibody and TO-PRO®3 (Invitrogen), a nuclear marker, for 30 min, mounted with ProLong® Gold Antifade reagent (Invitrogen), and then imaged with a laser confocal microscope (LSM710, Carl Zeiss). For immunohistochemistry, sections were incubated overnight with anti-glial fibrillary acidic protein (GFAP) mouse

monoclonal antibody (1:1000, Sigma-Aldrich), stained using the DAKO EnVision™+ HRP system (Dako Corp.) and photographed with an optical microscope (Axio Imager M1). The immunoreactive area in the ventral horn of TDP CKO mice and control littermates at the indicated ages ($n = 3$ for each age) was analysed with WinROOF (Mitani). The binary treatment included application of a staining intensity threshold and size exclusion criteria to distinguish the significant structures from the background signals. All sections analysed were treated with the same threshold and exclusion criteria.

Retrograde FluoroGold neurotracer labelling

Retrograde labelling of motor neurons was performed as described previously (Katsuno *et al.*, 2006). Briefly, a total volume of 4.5 µl of 2.5% FluoroGold solution (Biotium) was injected into the gastrocnemius muscle of anaesthetized mice. Lumbar spinal cords were removed 46 h after FluoroGold administration. The frozen optimal cutting temperature (OCT) compound-embedded samples were sectioned longitudinally on a cryostat at 10 µm and mounted on silane-coated slides. After the FluoroGold labelled motor neurons in the L5 segment was photographed with Zeiss Axio Imager M1 (Carl Zeiss), the sections were fixed with 4% paraformaldehyde, stained with anti-TDP-43 and anti-ChAT antibody, and photographed with LSM710. For the quantification of retrograde labelling, we measured every third section (a total of five sections in L5 ventral horn), and counted the degree of FluoroGold labelling in motor neurons of two control mice, and TDP-43-positive or -negative motor neurons of two TDP CKO mice.

Electron microscopy

Under the deep anaesthesia, 2-year-old TDP CKO mice and control littermates were transcardially perfused with 3% paraformaldehyde and 1% glutaraldehyde in PBS. The spinal cords and sciatic nerves were removed, and postfixed overnight in the perfusing solution. After fixation, the spinal cords were immersed in the solution (0.1 M cacodylic acid, 2% paraformaldehyde, 2.5% glutaraldehyde) for 12 h. The anterior half of lumbar spinal cord was sectioned transversely, postfixed in 1% osmium tetroxide for several hours, dehydrated and embedded in epoxy resin. Each block was cut into serial semithin sections (~1-µm thick). These sections were stained with toluidine blue. Appropriate portions of the sections were cut into ultrathin sections, which were then stained with uranyl acetate and lead citrate. Two-year-old TDP CKO mice and control littermates were analysed. Electron microscopic photographs were obtained under an original magnification of ×5000 and printed at a final magnification of ×9500.

Analysis of muscle, neuromuscular junction and motor axon

To investigate the presence of muscle atrophy, gastrocnemius muscles were dissected free, quickly frozen by immersion in cooled acetone and powdered CO_2. Ten-micrometre thick transverse frozen sections were stained with haematoxylin and eosin. For analysis of neuromuscular junctions, 30-µm thick frozen longitudinal sections of the tibialis anterior muscle were incubated overnight with alpha bungarotoxin conjugated with biotin-XX (1:80, Invitrogen), anti-pNF-H mouse monoclonal antibody (SMI31, 1:100) and anti-synaptophysin rabbit polyclonal antibody (1:100, Cell Signaling Technologies). After washing, sections were incubated with goat anti-rabbit and anti-mouse IgG conjugated with Alexa Fluor® 488 (1:1000 for each, Invitrogen) and streptavidin conjugated with Alexa Fluor® 564 (1:1000, Invitrogen) and mounted with ProLong® gold (Invitrogen). The stained sections were imaged with a laser scanning confocal microscope (LSM710, Carl Zeiss). More than 100 neuromuscular junctions from TDP CKO mice aged 20, 50, 80 and 100 weeks were analysed ($n = 3$ mice for each group). For morphological analyses, epoxy resin embedded transverse sections of L5 ventral roots were stained with toluidine blue. L5 ventral roots of 20, 50 and 100 week-old mice ($n = 6$ axons for each group) were assessed. The diameter of myelinated fibres was automatically measured using a computer-assisted image analyser (Luzex FS), as described previously (Katsuno *et al.*, 2002). Paraffin embedded transverse sections of L4 ventral roots of 100-week-old mice were stained with an antibody against ChAT and photographed by Zeiss Axio Imager M1.

Quantification and morphological analysis of motor neurons

For the quantifications and morphological analyses of motor neurons, we performed the immunofluorescent analyses of the paraffin-embedded sections stained with anti-TDP-43 and anti-ChAT antibodies of L5 spinal cord ($n = 5$ for each) and brain stem ($n = 3$ for each) of control and TDP CKO mice. All the neurons within the every fifth sections from the 50 consecutive sections of lumbar spinal cord, or every third sections from all consecutive sections of brain stem including the each cranial motor nucleus were assessed using AxioVision softwear (Carl Zeiss), after samples were photographed by Zeiss Axio Imager M1 (Carl Zeiss). The ChAT-positive neurons in the ventral horns or cranial nuclei were regarded as motor neurons. We examined the presence of nuclear immunoreactivity for TDP-43 in ventral horns and brainstems, and calculated the TDP-43-knockout efficiencies, the number of remaining motor neurons, and the size of motor neurons in each group. To evaluate the involvement of gamma-motor neuron, we measured the number of large ($>250\,\mu m^2$) or small ($<250\,\mu m^2$) lumbar motor neurons.

Statistical analyses

Statistical differences were analysed by Kaplan–Meier and logrank test for survival rate, ANOVA and Bonferroni *post hoc* analyses for multiple group comparisons and the unpaired Student's *t*-test for two group comparisons (SPSS version 15.0, SPSS Inc.).

Results

Generation of TDP CKO mice

We constructed a TDP-43flox allele by flanking the second exon of the mouse TDP-43 gene (*Tardbp*) with loxP sites (Supplementary Fig. 1A and B). Because the second exon contains the *Tardbp* start codon, Cre-mediated deletion of this exon inhibits mouse TDP-43 translation. To delete TDP-43 expression specifically in motor neurons, TDP-43$^{flox/flox}$ mice were crossed with VAChT-Cre.Fast mice, in which Cre expression is mostly restricted in the postnatal somatomotor neurons (Misawa *et al.*, 2003). The immunofluorescent analysis of the ventral horn from TDP CKO mice at post-natal Day 2 showed that all the assessed motor neurons were positive for TDP-43 (Supplementary Fig. 1C). On

the other hand, the quantitative analysis of the lumbar ventral horn and hypoglossal nucleus from 10-week-old TDP CKO mice showed that TDP-43 was knocked-out in 48% of motor neurons in the lumbar ventral horn and 45% in the hypoglossal nucleus (Fig. 1A and B). In addition, reverse transcriptase PCR analysis of total RNA from motor neurons isolated by laser microdissection, revealed that exon 2 of *Tarbdp* was partially skipped under the Cre expression (Supplementary Fig. 1D and E). Immunoblot analysis showed that the TDP-43 protein expressions in liver, kidney, heart, skeletal muscle and cerebral cortex of TDP CKO mice were not altered compared with their control littermates (Supplementary Fig. 1F). Immunofluorescent analysis of the

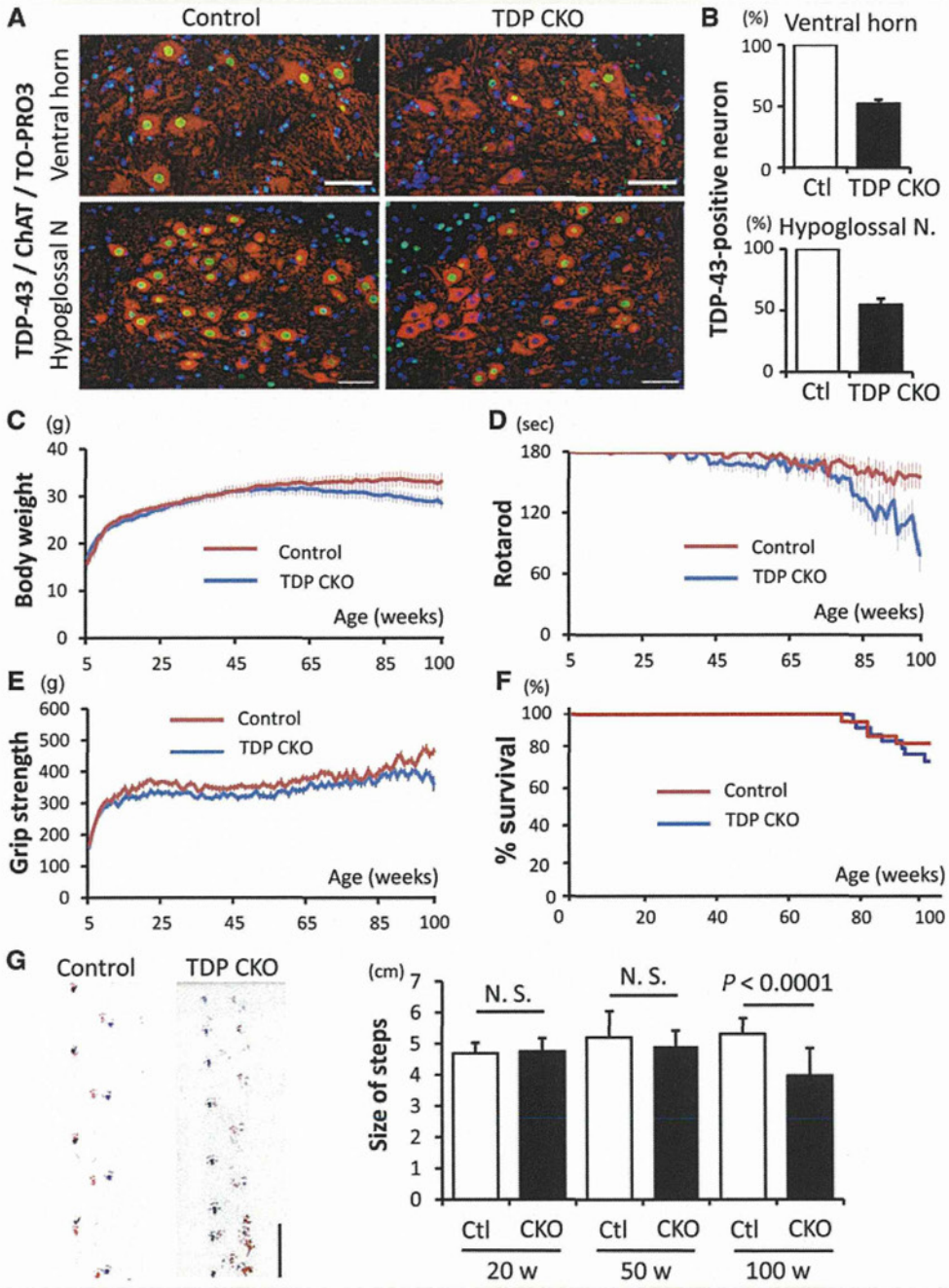

Figure 1 Progressive motor dysfunction in TDP CKO mice. (**A**) Immunofluorescent stainings (TDP-43; green, ChAT; red, TO-PRO3; blue) of lumbar ventral horn and hypoglossal nucleus of 10-week-old control and TDP CKO mice. (**B**) Percentage of TDP-43-positive motor neurons in the lumbar ventral horn and hypoglossal nucleus (N.) of 10-week-old control (Ctl) and TDP CKO mice ($n = 3$ for each group). (**C–E**) Body weight (**C**), Rotarod task (**D**), and grip strength (**E**) phenotypes of control (red line, $n = 21$) and TDP CKO mice (blue line, $n = 20$). Error bars indicate SEM. (**F**) Survival rates of control ($n = 27$) and TDP CKO mice ($n = 26$). (**G**) The average length of hindpaw steps in 20-week-old ($n = 6$ for each), 50-week-old ($n = 6$ for each), and 100-week-old ($n = 15$ for each) control and TDP CKO mice. Error bars indicate SD. Scale bars: **A** = 50 μm; **G** = 5 cm. N.S. = not significant.

lumbar dorsal horn of 10-week-old control, TDP CKO and TDP hCKO mouse showed that all the assessed neurons were positive for TDP-43 (Supplementary Fig. 2). In addition, the analyses of 100-week-old control, TDP CKO and TDP hCKO mice demonstrated that TDP-43 was not excised in the neurons of the primary motor cortex, putamen, deep cerebellar nucleus and cerebellar cortex of TDP CKO or TDP hCKO mouse (Supplementary Figs 3 and 4).

TDP-43 CKO mice develop progressive motor dysfunction

The earliest symptom of motor deficit in TDP CKO mice was tremor, which appeared as early as 50 weeks. TDP CKO mice exhibited progressive weight loss beginning ~60 weeks (Fig. 1C), when muscle atrophy of the trunk and hind limb was detectable. The grip strength and motor performances in the Rotarod task of TDP CKO mice were lower than their control littermates (Fig. 1D and E) beginning at 85 and 75 weeks, respectively. At 100 weeks, TDP CKO mice were significantly different from the control littermates in body weight ($P = 0.04$), rotarod ($P = 0.001$) and grip strength ($P = 0.002$). The average length of hindpaw steps of TDP CKO mice was significantly shorter than that of control littermates in 100 weeks of age ($P = 0.000001$; Fig. 1G). The survival rate of TDP CKO mice, however, was not altered compared with that of control littermates (Fig. 1F). Analyses of TDP-43$^{flox/+}$ and TDP-43$^{flox/+}$/VAChT-Cre (TDP hCKO) mice, which resulted in heterozygous loss of TDP-43 in motor neurons, showed that body weight, Rotarod task, grip strength and length of hindpaw steps were not significantly different between the two transgenic groups (Supplementary Fig. 5A–D).

TDP-43 depletion leads to atrophy of spinal motor neurons

Because TDP CKO mice exhibited progressive motor impairment, we focused on the morphology of spinal motor neurons. The immunofluorescent analysis of the lumbar ventral horn in 100-week-old TDP CKO mice revealed that motor neurons without TDP-43 were significantly smaller than those with TDP-43 and those in control littermates (Fig. 2A–C). Although TDP-43 was knocked-out in 49% of motor neurons in TDP CKO mice, the number of motor neurons in TDP CKO mice did not differ from that in control littermates (Fig. 2D and E). A time course analysis of TDP-43-lacking motor neurons in TDP CKO mice showed that neuronal atrophy was evident at 100 weeks (Fig. 2F). In addition, we measured TDP-43 knockout efficiency in the small ($>250\,\mu m^2$) and large ($<250\,\mu m^2$) lumbar motor neurons. The results showed that there was no difference in the knockout efficiency between the small and large motor neurons (Supplementary Fig. 6A), suggesting that the TDP-43-knockout efficiency in the gamma-motor neurons of TDP CKO mice is similar to that of alpha-motor neurons. The measurement of the average motor neuron number showed that the number of TDP-43-lacking large motor neurons decreased at 100 weeks of age compared with TDP-43-positive motor neurons, whereas the number of TDP-lacking small motor neurons increased, indicating that postnatal deletion of TDP-43 leads to atrophy of the alpha-motor neurons in the aged TDP CKO mice (Supplementary Fig. 6B). This view is supported

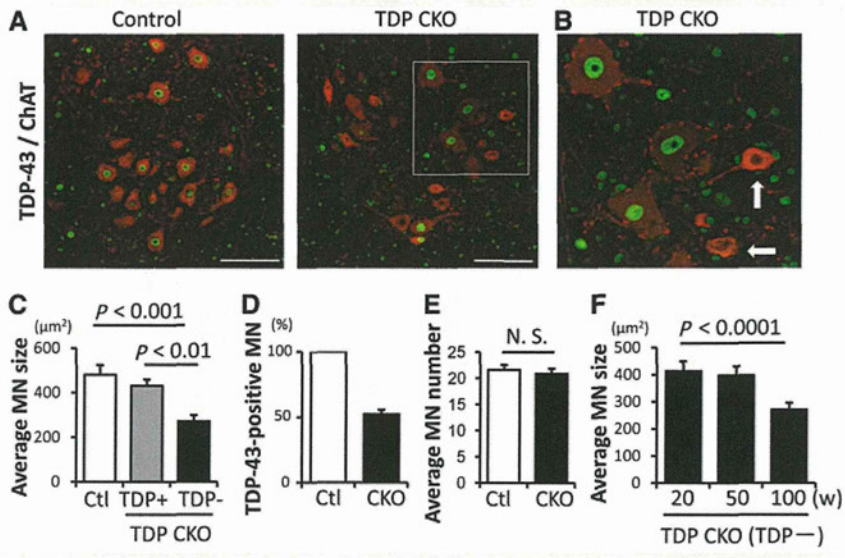

Figure 2 Morphological analysis of spinal motor neurons. (**A** and **B**) Immunofluorescencent stainings (TDP-43, green; ChAT, red) of lumbar ventral horn from 100-week-old control (Ctl) and TDP CKO mice. (**B**) Enlarged image of the area marked in **A** (*left*). TDP-43-lacking motor neurons (arrows) were significantly smaller than TDP-43-positive motor neurons. (**C**) Percentage of TDP-43-positive motor neurons in the lumbar ventral horn of 100-week-old mice ($n = 5$ for each group). (**D**) Average size of spinal motor neurons (MN) in 100-week-old mice ($n = 5$ for each group). Error bars indicate SD. (**E**) Average number of spinal motor neurons in 100-week-old mice ($n = 5$ for each group). Error bars indicate SD. (**F**) Time course of atrophy of TDP-43-lacking motor neurons ($n = 5$ for each age). TDP+ = TDP-43-positive neurons; TDP− = TDP-43-negative neurons. Scale bars = 100 μm.

by the immunofluorescent analysis of the lumbar ventral horn from 100-week-old TDP CKO mice showing that the TDP-43-lacking alpha-motor neuron, which was positive for NeuN and ChAT, was smaller than the TDP-43-positive alpha-motor neuron (Supplementary Fig. 6C). On the other hand, there was no morphological difference in the motor neurons between TDP hCKO and TDP-43$^{flox/+}$ mice (Supplementary Fig. 5E).

TDP-43 depletion affects motor axon, neuromuscular junction and skeletal muscle

The toluidine blue staining of transverse sections of L5 ventral root exhibited axonal degeneration in a subset of large myelinated fibres of TDP CKO mice from 50 weeks (Fig. 3A). Quantitative analyses of the ventral roots demonstrated the decrease of large myelinated fibres and increase of small myelinated fibres in 100 week-old TDP CKO mice (Fig. 3A). The immunofluorescent analysis using anti-ChAT antibody also exhibited the loss of large motor axons in the ventral root of TDP CKO mice (Fig. 3B). Axial sections of the gastrocnemius muscle in 100-week-old TDP CKO mice exhibited grouped atrophy, a neurogenic muscular change (Fig. 3C). Whereas all assessed neuromuscular junctions in the control littermates were innervated, in the TDP CKO mice, the percentage of denervated neuromuscular junctions increased progressively after the age of 50 weeks, concomitant with motor impairment and motor neuron atrophy (Fig. 3D). In analyses of retrograde FluoroGold labelling of the motor neurons in TDP CKO mice, the degree of labelling was significantly less in the TDP-43-lacking motor neurons than in the TDP-43-positive motor neurons (Fig. 3E).

Assessment in motor nuclei of cranial nerves

The histopathology of patients with ALS is characterized by the selective loss of motor neurons with scarcely detectable damage in the extraocular motor nuclei. To examine the region-specific neuropathology in TDP CKO mice, we quantitatively analysed the motor nuclei of cranial nerves. In the trigeminal motor, facial, hypoglossal and abductor nuclei of 100-week-old TDP CKO mice, ~50% of motor neurons were negative for TDP-43, but in the oculomotor nucleus, the efficiency of TDP-43 depletion was only ~25% (Supplementary Fig. 7). Morphological analysis of the trigeminal motor, facial and hypoglossal nuclei in 100-week-old TDP CKO mice revealed that TDP-43-lacking motor neurons were significantly smaller than those with TDP-43 or those of the control littermates (Fig. 4A–C), whereas those in the oculomotor and the abductor nuclei were preserved (Fig. 4D and E), suggesting that this mouse model recapitulates the selective vulnerability of motor neuron in ALS. The time course analysis of the hypoglossal motor nucleus showed that the atrophy of the motor neuron was evident from 50 weeks. The number of motor neurons in these nuclei of TDP CKO mice was not altered compared with the control littermates, as was shown in the spinal cord (Fig. 4A–E).

Astrogliosis in ventral horn and accumulation of phosphorylated neurofilament in motor neurons of TDP CKO mice

Immunohistochemistry of the ventral horn showed that the number of astrocytes progressively increased in TDP CKO mice (Fig. 5A). Phosphorylated neurofilament accumulated in the cytoplasm of TDP-43-lacking motor neurons of TDP CKO mice, but not in motor neurons with TDP-43 in TDP CKO mice or those of control littermates (Fig. 5B).

Formation of autophagosomes in motor neurons of TDP CKO mice

Recent studies indicate that autophagosomes accumulate in motor neurons of patients with sporadic ALS and animal models of motor neuron diseases (Li *et al.*, 2008; Sasaki, 2011; Tian *et al.*, 2011). Therefore, we investigated autophagy-related pathology in 100-week-old control and TDP CKO mice. The immunofluorescent analysis showed LC3-positive puncta in 37% of TDP-43-lacking motor neurons, but not in TDP-43-positive motor neurons in TDP CKO mice or those of the control littermates (Fig. 6A). TDP-43-lacking motor neurons with the puncta were significantly smaller than those without the puncta (Fig. 6B). The ultrastructure of motor neurons from 100-week-old TDP CKO mice demonstrated that autophagy-related structures such as autolysosomes and autophagosomes were accumulated in the cell bodies of motor neurons (Fig. 6C–E), proximal motor axon (Fig. 6F), and sciatic nerve of TDP CKO mice (Fig. 6G–H). These structures were not seen in the control mice as far as we observed.

Discussion

Although TDP-43 is an established pathological hallmark of ALS, it remains unclear how TDP-43 contributes to the pathogenesis. In the present study, we showed that TDP CKO mice, in which TDP-43 was knocked-out specifically in postnatal motor neurons, developed an age-dependent progressive motor impairment such as gait disturbance and muscle atrophy, suggesting that the loss-of-function of TDP-43 in postnatal motor neurons plays a causative role in the neurodegenerative process of ALS. There has been a great deal of debate about whether loss or gain of TDP-43 function causes the neurodegeneration (Lee *et al.*, 2011). Several mouse, rat and primate models overexpressing wild-type or disease mutant TDP-43 recapitulate the phenotype of ALS or FTLD (Wegorzewska *et al.*, 2009; Shan *et al.*, 2010; Stallings *et al.*, 2010; Tsai *et al.*, 2010; Wils *et al.*, 2010; Xu *et al.*, 2010; Zhou *et al.*, 2010; Igaz *et al.*, 2011; Swarup *et al.*, 2011; Uchida *et al.*, 2012); however, redistributions and cytoplasmic inclusions of TDP-43 are generally rare and several models exhibit cytoplasmic mitochondrial aggregation, which is not common in ALS. The expression of endogenous TDP-43 is suppressed in neurons expressing human TDP-43-delta nuclear localization signal as well as those expressing human wild-type TDP-43, suggesting that

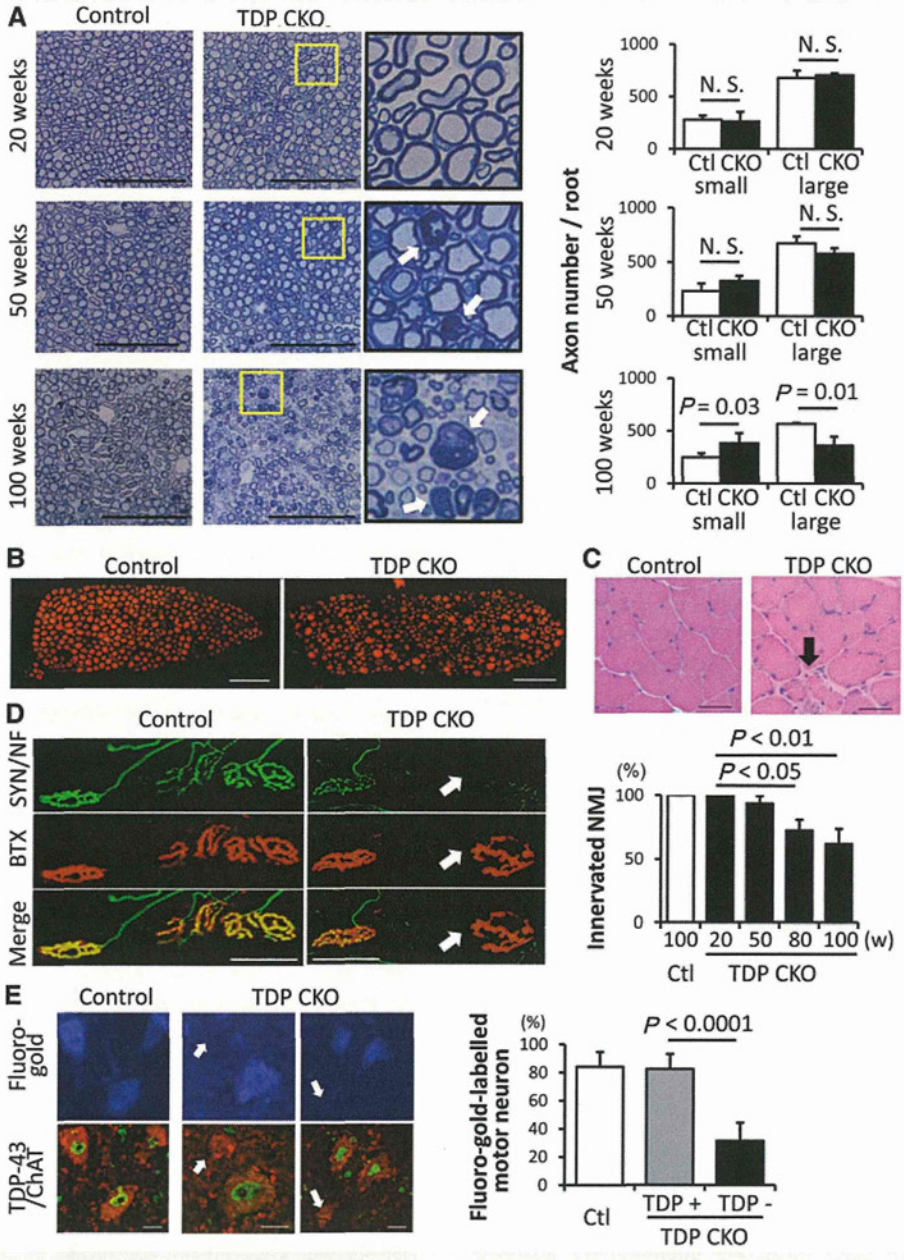

Figure 3 Analysis of motor axons, neuromuscular junctions, and skeletal muscles. (**A**) Toluidine blue staining images and the number of small myelinated fibres (<5 μm) and large myelinated fibres (>5 μm) in the L5 ventral root from 20, 50 and 100-week-old control and TDP CKO mice (n = 6 axons of each). The enlarged image of the yellow-framed area is also shown. Arrows indicate axonal degenerations. Scale bars = 100 μm. Error bars indicate SD. (**B**) Immunofluorescent staining of the L4 ventral root in 100-week-old mice with an anti-ChAT antibody. (**C**) Haematoxylin and eosin staining of gastrocnemius muscles of 100-week-old mice. Axial sections from TDP CKO mice exhibited grouped atrophy (arrow), whereas the control littermates showed no such phenomenon. (**D**) Immunofluorescent staining [synaptophysin (SYN) and phospho-neurofilament (NF), green; bungarotoxin (BTX), red] of neuromuscular junctions (NMJ) in 100-week-old mice and a time course analysis of neuromuscular junctions in TDP CKO mice. Denervated neuromuscular junctions (arrow) are indicated by the lack of synaptophysin and phospho-neurofilament staining. Scale bars = 50 μm. Error bars indicate SD (n = 3). (**E**) FluoroGold labelling (blue) and immunofluorescence staining (TDP-43, green; ChAT, red) of lumbar motor neurons. Retrograde FluoroGold labelling was significantly attenuated in TDP-43-lacking motor neurons but not in TDP-43-positive neurons in 100-week-old TDP CKO mice (arrows). Scale bars = 20 μm. Error bars indicate SD (n = 10).

mutant TDP-43 may cause neurodegeneration through inhibition of normal TDP-43 function (Igaz *et al.*, 2011). On the other hand, TDP-43 knockout mice result in embryonic lethal phenotypes (Kraemer *et al.*, 2010; Sephton *et al.*, 2010; Wu *et al.*, 2010), and systemic postnatal deletion of this molecule led to rapid death (Chiang *et al.*, 2010). Although TDP-43-depleted models of *Drosophila* and zebrafish exhibit neurodevelopmental deficits in motor axons (Feiguin *et al.*, 2009; Kabashi *et al.*, 2011), the